Density Fluctuations and Energy Spectra of 3D Bacterial Suspensions Supplemental Material

Zhengyang Liu, Wei Zeng, Xiaolei Ma, and Xiang Cheng
Department of Chemical Engineering and Materials Science, University of Minnesota, Minneapolis, MN 55455, USA
(Dated: December 19, 2020)

I. EXPERIMENT DETAILS

A. Light-powered *E. coli*

We introduce a light-driven transmembrane proton pump, proteorhodopsin (PR), to wild-type *E. coli* (BW25113) by transforming the bacteria with plasmid pZE-PR encoding the SAR86 γ-proteobacterial PR-variant (Walter 2007). The activity of PR is correlated with the intensity of light. Thus, we can control the swimming speed of bacteria using light of different intensities. In our experiments, we use high-intensity light, which saturates the light response of bacteria. The average swimming speed of bacteria is fixed at $v_0 = 15 \pm 3$ μm/s in the dilute limit.

The bacteria are cultured at 37 ℃ with a shaking speed at 250 rpm for 14-16 hours in terrific broth (TB) [tryptone 1.2% (w/w), yeast extract 2.4% (w/w), and glycerol 0.4% (w/w)] supplemented with 0.1 g/L ampicillin. The culture is then diluted 1: 100 (v: v) in fresh TB and grown at 30 ℃ for 6.5 hours. PR expression is triggered by supplementing the culture medium with 1 mM isopropyl β-D-thiogalactoside and 10 μM ethanolic all-trans-retinal in the mid-log phase (3 hours after the dilution).

The bacteria are harvested by gentle centrifugation (800g for 5 min). After discarding the culture medium in the supernatant, we resuspend bacteria with DI water. The resuspended suspension is then centrifuged again at 800g for 5 min, and finally adjusted to the target concentration for experiments.

II. SAMPLE PREPARATION AND MICROSCOPY

To prepare the sample for microscopy, we construct a seal chamber made of glass slides (25 mm × 75 mm) and coverslips (18 mm × 18 mm). We first glue (NOA 81, Norland, NJ) two coverslips on a glass slide, side-by-side, leaving a 3-mm separation between the two coverslips. We then cover the 3-mm separation with another coverslip to form a channel. We then pipette bacterial suspensions into the channel. Finally, we seal the two ends of the channel using UV glue (NOA 76, Norland, NJ) to form a sealed chamber.

Images of the bacterial suspensions are taken 50 μm above the bottom surface of the sealed chamber by a Nikon Ti-E inverted microscope using the bright field mode and a 20× (NA 0.5) objective. The field of view is 420 × 360 μm^2. All videos are recorded at 30 frames per second using a sCMOS camera.

III. IMAGE ANALYSIS DETAILS

A. Calculation of density fluctuations

Please rewrite/reorganize this section. I combine this session with the session on the normalization of GNF. The two sessions together allow you to convert I into N eventually. Using the TVSA method, we first crop square-shape subsystems of various sizes from the original image time series, as shown in Fig. 1a. For each size l, a standard deviation of the light intensity ΔI are calculated over time. What you directly measure is the image intensity. I suggest we use ΔI and I first and state clearly how ΔI and I are related to ΔN and N at the end. To improve statistics, we choose 20 different subsystems of the same size evenly distributed in the field of view and obtain an average ΔI and I (Fig. 1b). We vary the subsystem size l from 10 μm to 30 μm, from 10 to 30 um? It seems to be a very small range. and examine the temporal variations of image intensity $\Delta I_i(l)$ in the i^{th} frame for subsystem size l. The temporal variations are then averaged in space (over i) to give the final ΔI. I am confused that if i is the number of frame, why is it an average of space? Since I is linearly proportional to bacterial volume fraction ϕ. $\Delta I \sim \Delta\phi$ Then number fluctuations in the system is captured by the dependence of ΔN_j on l_j. In an equilibrium system, $\Delta N_j \propto l_j$ (this follows from $\Delta N_j \propto \sqrt{N_j}$ and $N_j \propto l_j^2$). Thus, the deviation from $\Delta N_j \propto l_j$ quantifies the giant number fluctuation in the system. In the main paper, we plot $\Delta N_j/l_j$ as a function of l_j^2/l_b^2, where l_b is the length scale of single bacterial body length, chosen to be 3 μm. To be consistent with the notations in literatures, we get rid of the subscript j, and write l_j as $\sqrt{N}$. Note that the subscript j denotes different choices of box sizes.

Without a more careful calibration, we are not able to obtain the exact number of particles using this Beer's law based method. Fortunately, the calculations of GNF does not require the exact number, but only the relative number. In the main paper, we show that the volume fractions ϕ and average pixel intensities I follow a pretty linear relation. Such a relation entails that $\Delta I \propto \Delta N$, which is followed by $\Delta I/\sqrt{N} \propto \Delta N/\sqrt{N}$. The proportionality allows us to get the scaling exponents of

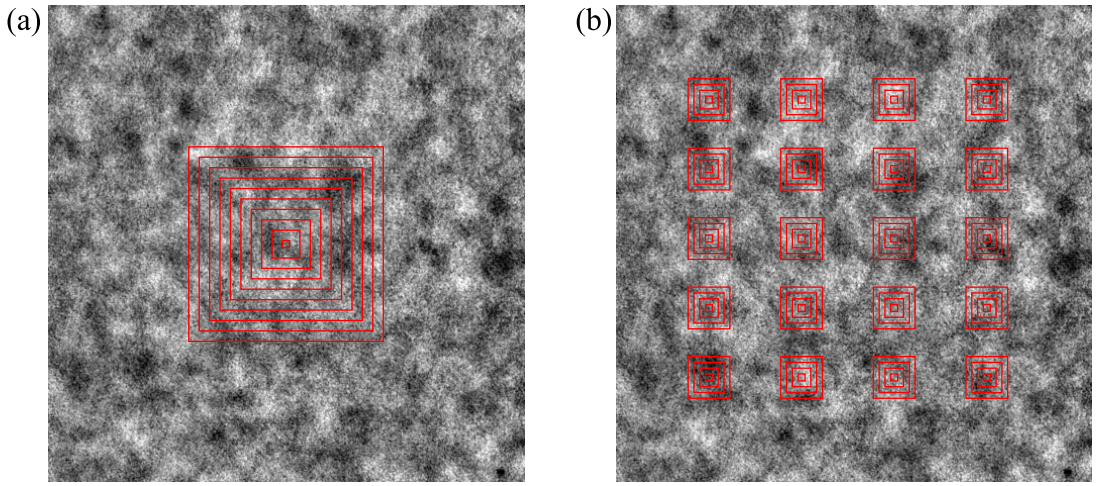

FIG. 1. **GNF calculations.** (a) Varying subsystem sizes. (b) Multiple seeds of subsystems for spatial average.

$\Delta N/\sqrt{N}$ against N, without having to measure the exact particle numbers.

In Fig. 1d, we show that under the same illumination and imaging condition, the density and average pixel intensity follow approximately a linear relation, which can be expressed as suggests:

$$\phi = a + bI \tag{1}$$

where ϕ is the volume fraction of bacterial suspensions, I is the average pixel intensity in a window, a and b are constants under the same illumination and imaging conditions. The number of bacteria in a given subsystem with side length l and thickness d can be calculated as

$$N = \frac{\phi l^2 d}{V_b} \tag{2}$$

where V_b is the volume of a single bacterium. Take the standard deviation of both sides of Eq. 4, we get

$$\Delta N = \frac{|b|d}{V_b} l^2 \Delta I \tag{3}$$

where Δ stands for taking the standard deviation over time. Over different length scales and volume fractions, $\frac{|b|d}{V_b}$ is a constant.

The number fluctuations $\Delta N/\sqrt{N}$ we present in the main text is actually $\Delta I/l$, where l is the length of subsystem size. These two values are proportional because

$$N = \frac{\phi l^2 d}{V_1} \tag{4}$$

where V_1 is single cell volume. The standard deviation ΔN is

$$\Delta N = |b| \Delta I \frac{d}{V_1} = \frac{|b|d}{V_1} \Delta I \tag{5}$$

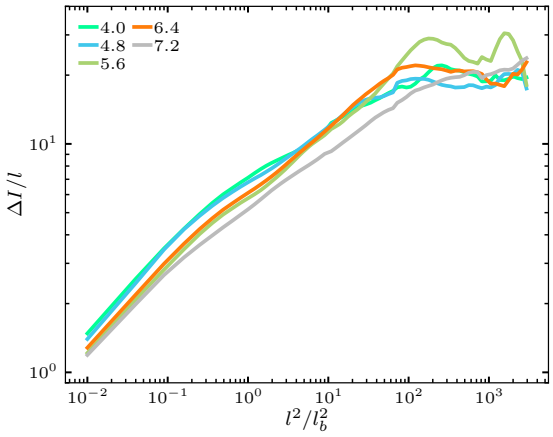

FIG. 2. **GNF curves at various volume fractions under same illumination and imaging conditions.**

from Eq. 4 and 5, we have $N \propto l$ and $\Delta N \propto \Delta I$. The proportionality allows us to extract the scaling exponents α, but prevents us from comparing the magnitudes of GNF across different volume fractions, due to the change in illumination and imaging conditions.

To illustrate the effect of changing imaging conditions, we measure the GNF of the same sample, under the same illumination, and use both 1 ND filter and 2 ND filter under the objective to dimmer the light that goes to the camera. Note that we have to use at least one filter to avoid over exposure of the camera. The result is shown in Fig. **??**, where all the four runs with 2 filters falls into a bundle, where as the run with only one filter clearly lies out of the bundle. Despite the big difference in the magnitude, the overall length scale dependence is quite similar, suggesting that measuring GNF using light in-

tensity is valid.

In order to compare the magnitude of GNF across different volume fractions, and more importantly compare GNF with energy spectra, we need to normalize the GNF curves obtained at different illumination and imaging conditions, so that they reflect the actual relative magnitude independent of illumination and imaging conditions. To do it, we use the same illumination and imaging conditions to take videos of bacterial suspensions at various volume fractions where we control all the imaging parameters strictly. The results are shown in Fig. 2, where all the curves are very close at small length scale, and show deviation at large length scales. This observation is intuitive: small scale density fluctuations is determined primarily by single cell dynamics and is not a strong function on volume fractions.

In the main text, we normalized all the GNF curves at small length scale, by forcing them to start from 1.

B. Particle image velocimetry (PIV)

2D in-plane velocity fields are extracted by Particle Image Velocimetry (PIV) analysis using openPIV package in Python Reference. We fix the box size to be 16 μm, which is larger than the size of a single bacterial body but smaller than the velocity correlation length. A step size of the half of the box size (8 μm) is used by convention, which sets the spatial resolution of the velocity fields.

C. Energy spectra

The energy spectra of bacterial suspensions are calculated as follows.

Again, we need to show how the calculation is actually performed, instead of the theory behind. For example, we should state how we use FFT on the PIV velocity data and how the results are related to $E(k_x, k_y)$. Finally, we should discuss how $E(k_x, k_y)$ is used to finally get $E(k)$.

$$E(k_x, k_y) = \frac{\langle u_k(k_x, k_y) u_k^*(k_x, k_y) + v_k(k_x, k_y) v_k^*(k_x, k_y) \rangle}{2A} \tag{6}$$

where E is the energy density in k space, u_k and v_k are k space velocity fields, A is the real space area of the system and * denotes the complex conjugate. The $\langle \cdot \rangle$ denotes an average over multiple images from different times. This method can be shown to be equivalent to another commonly used formula, which calculates the Fourier transform of real space velocity spatial correlation functions:

$$E^1 = \int \langle \boldsymbol{u}(\boldsymbol{r_0}) \boldsymbol{u}(\boldsymbol{r_0} + \boldsymbol{r}) \rangle e^{-i\boldsymbol{k}\cdot\boldsymbol{r}} d\boldsymbol{r} \tag{7}$$

it is good to document the following derivation somewhere (maybe in your thesis), but we don't need to show it in the paper.) We show here how they are equivalent by considering one of the velocity componenet u. Starting with the definition of E

$$\begin{aligned} E(k_x, k_y) &= u_k(k_x, k_y) u_k^*(k_x, k_y) \\ &= \iint u(x, y) e^{-ik_x x} e^{-k_y y} dx dy \left[\iint u(x', y') e^{-ik_x x'} e^{-ik_y y'} d \right. \\ &= \iint u(x, y) e^{-ik_x x} e^{-k_y y} dx dy \iint u^*(x', y') e^{ik_x x'} e^{ik_y y'} dx' d \\ &= \iiiint u(x, y) u(x', y') e^{-ik_x (x - x')} e^{-k_y (y - y')} dx dy dx' dy' \end{aligned} \tag{8}$$

here, we change variable and let $x'' = x - x'$ and $y'' = y - y'$ the original expression can be rearranged into

$$\begin{aligned} &\iiiint u(x' + x'', y' + y'') u(x', y') e^{-ik_x x''} e^{-k_y y''} d(x' + x'') d(y' + y'') \\ &= \iint \left[\iint u(x' + x'', y' + y'') u(x', y') dx' dy' \right] e^{-ik_x x''} e^{-k_y y''} d(x' + \end{aligned} \tag{9}$$

using the definition of velocity correlation function (average all possible pairs over available space):

$$\langle u(x, y) u(x + x'', y + y'') \rangle = \frac{\iint u(x' + x'', y' + y'') u(x', y') dx' dy'}{\iint dx' dy'} \tag{10}$$

we obtain

$$\iint dx' dy' \iint \langle u(x, y) u(x + x'', y + y'') \rangle e^{-ik_x x''} e^{-k_y y''} dx'' dy'' \tag{11}$$

the first integration is the available space size of velocity field, in this case the system area A. Thus,

$$E(k_x, k_y) = E^1(k_x, k_y) \tag{12}$$

D. Correlation of local density fluctuations and kinetic energies

We need more details. In addition to the definition of the correlation function, we need to show how the density fluctuations and kinetic energies are calculate at $l = 2.5 l_b$, staring from pixel image intensity and velocity fields at 8 um spacing. The cross correlation calculation used when analyzing the local correlation between kinetic energy and density fluctuations is defined as the following:

$$A \star B = \frac{\langle (A - \bar{A})(B - \bar{B}) \rangle}{\sigma_A \sigma_B} \tag{13}$$

where A and B are two arrays of scalars, $\star$ is the operator standing for cross correlation, $\bar{\cdot}$ means taking the mean, σ means the standard deviation, and $\langle \cdot \rangle$ denotes taking the average of all scalars in an array. The cross correlation quantifies the similarity between arrays A and B. The resulting number takes value from -1 to 1.

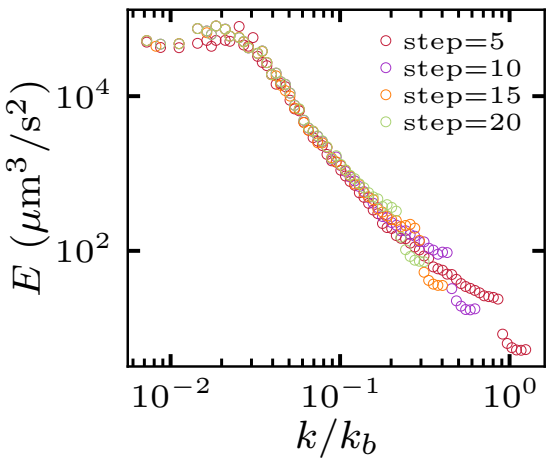

FIG. 3. **Energy spectra of the same active turbulence, measured at different PIV step size.**

E. Density fluctuations in the transient state

This session is necessary. I have not worked on the revision of the session yet though. When calculating the local density fluctuations, we want to measure the instantaneously change of density instead of a steady-state scaling. Thus, we choose the length of video for this calculation to be within the autocorrelation time of density (or more accurately, average pixel intensity) variations. We also want to include as many frames as we can instead of using adjacent frame, in order to suppress the effects from random fluctuations of image intensities, the nature of optical imaging.

We first calculate the autocorrelation functions of density. The basic principle of this calculation is to shift a time series of density at varying steps and calculate the matching between the original series and the shifted series, using the cross correlation scheme as in Eq. 13. In Fig. **??**, we plot the autocorrelation function of density at various volume fractions, covering the range studied in this work. We notice that low volume fraction suspensions display a longer correlation time. The smallest correlation time, according to this measurement, is around 1 second, which corresponds to 30 frames in our videos. Thus, we choose 10 frames as the video length for calculating the local density fluctuations, which is much smaller than the correlation time but still has many enough frames to suppress the random flucutations from imaging.